Eur. Phys. J. B **18**, 625–632 (2000)

THE EUROPEAN PHYSICAL JOURNAL B

EDP Sciences

Neutron scattering on the strongly correlated electron $CeNi_{1-x}Cu_x$ system: from non-magnetic behaviour to long-range magnetic order

J.I. Espeso[1,a], J. García Soldevilla[2], J.A. Blanco[3], J. Rodríguez Fernández[2], J.C. Gómez Sal[2], and M.T. Fernández Díaz[4]

[1] Dpto. Física Moderna, Universidad de Cantabria, 39005 Santander, Spain
[2] CITIMAC, Universidad de Cantabria, 39005 Santander, Spain
[3] Dpto. de Física, Universidad de Oviedo, 33007 Oviedo, Spain
[4] Institut Laue Langevin, BP 156, 38042 Grenoble Cedex, France

Received 22 May 2000

Abstract. The ground state of the strongly correlated electron $CeNi_{1-x}Cu_x$ compounds has been investigated by means of neutron scattering experiments. Thus, magnetic diffraction was performed for compounds showing long-range magnetic order ($x > 0.2$). An evolution from a collinear ferromagnetic structure for $x = 0.6$ to a simple antiferromagnetic one for CeCu takes place through some more complex magnetic structures for intermediate compositions. The magnetic moments are continuously reduced when the Ni content increases reflecting the progressive enhancement of the Kondo screening. The large reduction found for $x = 0.6$ compound is discussed and the existence of a spin glass like component of the magnetic moment cannot be discarded. From the quasielastic spectra, we have obtained the Kondo temperatures which are close to the magnetic ordering ones. The quasielastic line-width evolves from a linear temperature dependence to a $T^{1/2}$ behaviour when approaching the non-magnetic limit. Then, this system provides an interesting example for the evolution of unstable $4f$ shell relaxation regimes when modifying the hybridisation strength.

PACS. 75.25.+z Spin arrangements in magnetically ordered materials (including neutron and spin-polarized electron studies, synchrotron-source x-ray scattering, etc.) – 75.30.Mb Valence fluctuation, Kondo lattice, and heavy-fermion phenomena

1 Introduction

In many cerium compounds the separation between intermediate valence, non-magnetic ground states with Fermi or non-Fermi liquid behaviour, heavy fermion and Kondo lattice systems is neither very well-defined nor an easy task. In these systems, the $4f$-conduction band hybridisation originates strong and rapid charge and spin fluctuations of the ground state, favouring the formation of non-magnetic ground states and leading to the appearance of the so-called "Kondo effect" phenomenology. The degree of hybridisation is usually parameterised by the Kondo temperature, T_K. Furthermore, in most of these systems, the Rudermann-Kittel-Kasuya-Yosida (RKKY) interaction, represented by the critical ordering temperature T_c, is altered by the Kondo effect. In addition, in rare-earth compounds the Crystalline Electric Field (CEF) anisotropy takes on a fundamental role in determining the magnitude and direction of the magnetic moments.

Neutron scattering techniques have provided a powerful microscopic tool for the understanding of strongly correlated electron systems due to their unique capability of proving local magnetic properties [1,2]. On the one hand, neutron diffraction studies allow characterising the long-range magnetic order and determining the reduction of the total magnetic moment due to hybridisation effects [3]. On the other hand, depending on the energy transfer range ($\hbar\omega$), the inelastic neutron scattering provides different kinds of information. In fact, for $\hbar\omega$ far away from the elastic contribution we can obtain information on local one-site (CEF) or collective (phonons and magnons) excitations, while for the quasielastic contribution ($\hbar\omega$ quite close to the elastic peak) a broad quasielastic line can be observed. In this case, the half-width at half-maximum ($\Gamma/2$), is related to the Kondo temperature and its variation with temperature depends on the magnetic state. For intermediate valence compounds, the quasielastic peak is broad and $\Gamma/2$ is almost temperature independent (as in $CePd_3$, $CeSn_3$ and $CeBe_{13}$ [4,5]) whereas in the case of Kondo lattice compounds, $\Gamma/2$ is smaller and two kinds

[a] e-mail: espesoji@unican.es

of temperature dependence have been found: a $T^{1/2}$ law usually found in non magnetic systems as $CeAl_3$ [6] and $CeCu_2Si_2$ [7] and a linear behaviour which corresponds to systems presenting long-range magnetic order (CeB_6 [8], $CeMg_3$ [9] and $CeNi_xPt_{1-x}$ [10]). However, in many cases the experimental data are not clear enough or do not cover enough temperature range to distinguish between those behaviours, and then this classification must be considered as merely orientative. These laws are supported by theoretical models based on different initial situations [11–13].

In order to get a better insight into the problem it is highly desirable to have a system exhibiting a continuous evolution between the magnetic and non-magnetic limits. This situation is fulfilled by the $CeNi_{1-x}Cu_x$ series. In fact, this system appears as an outstanding example to study the competition between inter-site RKKY exchange interactions and single site hybridisation effects in the presence of strong magnetocrystalline anisotropy. Starting from CeNi, an intermediate valence compound crystallizing in the orthorhombic CrB-type structure [14], a 10% substitution of Ni by Cu changes the crystalline structure to the FeB-type [15]. Previous magnetic measurements have shown that the composition with $x = 0.2$ does not present long-range magnetic order down to 1 K. The intermediate compositions ($0.4 \leq x \leq 0.8$) show a ferromagnetic (FM) order with a Curie temperature close to 1 K. For $x \geq 0.9$ a change to an antiferromagnetic (AFM) behaviour appears [15,16]. This change from FM to AFM ordering is similar to that observed in other isomorphous rare-earth $RNi_{1-x}Cu_x$ compounds [17–19]. On the other hand, $4f$-conduction band hybridisation effects decrease with increasing Cu content [16] due to the increasing interatomic distances as was also observed in the $CeNi_xPt_{1-x}$ series [20]. A crossover from a non-localised (non-magnetic) to a localised (magnetic) state appears close to 20% Cu. Thus, the intermediate compositions with $0.2 < x < 0.8$ are a new example of the few existing Kondo FM compounds [16].

In addition, it has recently been shown that the increasing hybridisation and the substitutional Ni/Cu disorder seems to be responsible for the existence and stability of a spin glass like behaviour in the $CeNi_{1-x}Cu_x$ FM compounds above T_c, leading to a complex magnetic phase diagram for this series [21].

In this paper we present the neutron scattering study in the $CeNi_{1-x}Cu_x$ series. We have determined the magnetic structures discussing the influence of the Cu substitution on the character of the observed magnetic arrangements and special attention has been paid to investigating the quasielastic contribution to the neutron scattering spectra. In this case, the results are discussed considering the theoretical models mentioned above [11–13].

2 Experimental details

Polycrystalline $CeNi_{1-x}Cu_x$ samples were melted in an arc furnace and the Cu rich ones $x > 0.6$ were annealed for one week at 425 °C under high vacuum to enhance the crystallinity of the samples. Their quality was checked by X-ray and neutron diffraction experiments and from both measurements only small traces (<5%) of $CeCu_2$ impurity phase were observed for the Cu rich compositions $x = 0.9$ and $x = 1$. X-ray and neutron diffraction data were analysed using the Rietveld method with the Fullprof program [22]. The macroscopic homogeneity of the samples was checked by X-ray dispersive analysis.

Table 1. Cell parameters and volume data obtained from the Rietveld refinements of the neutron diffraction patterns at low temperatures for the $CeNi_{1-x}Cu_x$ series ($x = 0.6$ and 0.8 at 5 K, $x = 0.9$ and 1 at 10 K).

x	a(Å)	b(Å)	c(Å)	V(Å^3)	R_{Bragg}(%)
0.6	7.316(3)	4.486(1)	5.641(2)	185.1(2)	4
0.8	7.386(6)	4.532(4)	5.656(4)	189.3(5)	10
0.9	7.412(6)	4.555(3)	5.645(4)	190.6(4)	9
1	7.415(4)	4.564(2)	5.643(3)	191.0(3)	4

Neutron scattering experiments were done at the Institut Laue Langevin (Grenoble, France). Neutron diffraction was performed at the D1B instrument using a dilution cryostat down to 100 mK and a standard cryostat. Powdered sample masses varied between 10 and 15 g.

Quasielastic neutron scattering experiments were performed at the time-of-flight spectrometer IN6. In the latter, the neutron incident energy was fixed at 3.15 meV, giving access to a momentum transfer of $0.42 < Q < 1.19$ Å^{-1}. The temperature was varied in the range 1.7–50 K. In this case, the sample masses were about 30 g.

3 Neutron diffraction: magnetic structures

3.1 Experimental results

All the studied samples, $x = 0.6$, 0.8, 0.9 and 1, crystallise in the orthorhombic FeB-type structure. Table 1 shows the evolution of the cell parameters obtained from the Rietveld refinements of the diffraction patterns at low temperature. The cell volume increases continuously with increasing Cu percentage. The **a** and **b** cell parameters also increase, while **c** remains almost constant.

Figure 1 shows the magnetic intensities (difference patterns 0.1–5 K) for $CeNi_{0.4}Cu_{0.6}$. The inset shows the difference pattern for $CeNi_{0.2}Cu_{0.8}$. For the ferromagnetic compound $x = 0.6$ the Rietveld analysis leads to a simple collinear arrangement below $T_c = 1$ K with the magnetic moments of the four Ce ions within the unit cell along the **b**-axis. The magnetic moment value of 0.6 μ_B at 0.1 K [23] is strongly reduced compared to that of the Ce^{3+} free ion one (2.14 μ_B). It is worth mentioning that in the isomorphous $NdNi_{1-x}Cu_x$ series the obtained magnetic moment for the ferromagnetic compound with $x = 0.6$ is 2.7 μ_B, which is slightly reduced with respect to the Nd^{3+} free ion value (3.27 μ_B). This reduction in the Nd based compounds is attributed to CEF effects [24].

The magnetic pattern of $CeNi_{0.2}Cu_{0.8}$ shows the coexistence of two propagation vectors. One, $\mathbf{q}_1$=0, corresponding to a ferromagnetic structure. In this case,

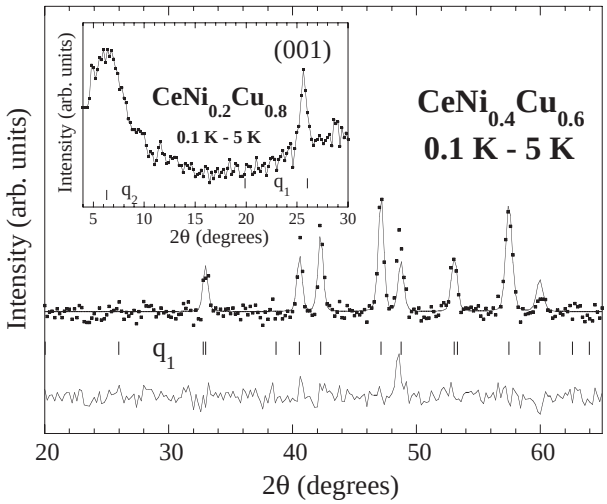

Fig. 1. Magnetic contribution to the neutron diffraction pattern for $CeNi_{0.4}Cu_{0.6}$ and $CeNi_{0.2}Cu_{0.8}$ compounds. Points indicate the experimental data and lines are the calculated and difference patterns. Vertical ticks mark the magnetic reflections: $|\mathbf{q}_1| = 0$ and $|\mathbf{q}_2| = 0.3$ Å^{-1}.

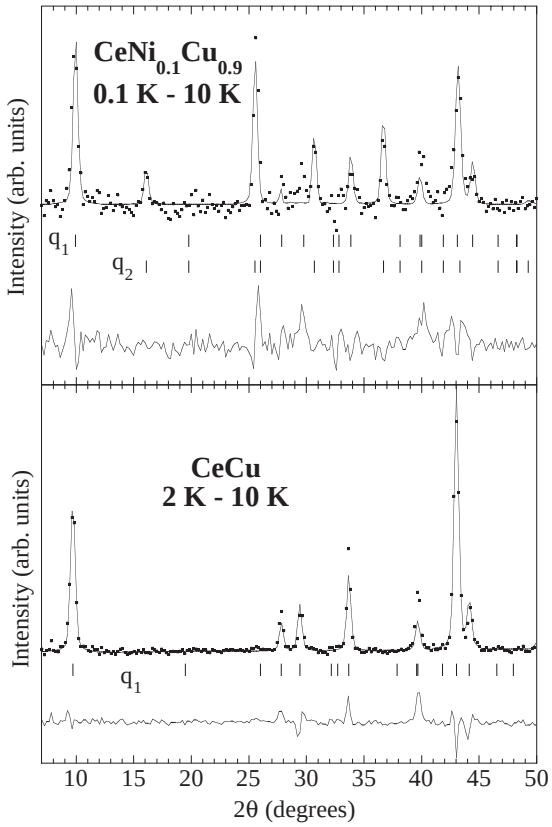

Fig. 2. Magnetic contribution to the neutron diffraction patterns for $CeNi_{0.1}Cu_{0.9}$ and CeCu compositions. Points indicate the experimental data and lines are the calculated and difference patterns. Vertical ticks mark the magnetic reflections: $\mathbf{q}_1$=(1/2,0,0) and $\mathbf{q}_2$=(0,1/2,0).

the existence of magnetic contribution corresponding to the (0,0,1) reflection, forbidden by the selection rules of the FeB nuclear structure, indicates that this ferromagnetic structure is non-collinear. Furthermore, a low angle peak also appears and it can be indexed with an incommensurate propagation vector of modulus $|\mathbf{q}_2| = 0.30$ Å^{-1}. The large width of this low angle peak suggests the existence of magnetic inhomogeneities in this incommensurate phase. The total magnetic structure has then a conical character; however, one should note that the absence of other additional magnetic peaks prevents a further quantitative analysis.

On the other hand, the magnetic structures of the AF compounds are quite complex. The magnetic patterns for the compound with $x = 0.9$ presents at 0.1 K two coexisting propagation vectors $\mathbf{q}_1$=(1/2,0,0) and $\mathbf{q}_2$=(0,1/2,0) (see Fig. 2). The best Rietveld refinement leads to a magnetic moment of 1.0 μ_B for both propagation vectors with the magnetic moments lying on the **ac** and **ab** plane for $\mathbf{q}_1$ and $\mathbf{q}_2$ respectively. The coexistence of these two propagation vectors, which are not equivalent by symmetry, is quite puzzling. Further experiments on single crystals under magnetic field or uniaxial stress are needed to distinguish between the existence of separate magnetic phases or a double-**q** magnetic structure. In contrast, the magnetic diffraction pattern of CeCu (Fig. 2) is indexed with a single propagation vector $\mathbf{q}_1$=(1/2,0,0). The best agreement at 2 K ($T/T_c = 0.6$) between the observeand calculated intensities is obtained with a magnetic moment of 1.45 μ_B lying in the **ac** plane. According to the temperature dependence of the magnetic moment a value of 1.8 μ_B at 0 K will be expected. The angles of the four Ce^{3+} magnetic moments with the **a**-axis in the unit cell are gathered in Table 2 together with a summary of the magnetic structures data obtained from the refinement of the diffraction patterns for this series. A schematic representation of the evolution of the magnetic moment arrangement along the series is displayed in Figure 3.

3.2 Discussion on magnetic structures

The first comment dealing with the magnetic structure data is about the progressive reduction of the Ce magnetic moment from CeCu (1.8 μ_B) to $CeNi_{0.4}Cu_{0.6}$ (0.6 μ_B). This reduction can be essentially due to two different reasons: $4f$-conduction band hybridisation (increasing Kondo screening) or CEF effects. For CeCu the magnetic moment reduction is about 10% with respect to that of the Ce^{3+} free ion value. This reduction is similar to that obtained for the isomorphous NdCu compound and then it can be mainly attributed to CEF effects. For an orthorhombic symmetry, the Ce^{3+} ground state ($J = 5/2$) is split into 3 doublets by the CEF. Then, the ground state is a mixture of some of the $M_J = \pm 5/2, \pm 3/2$ and $\pm 1/2$. In order to account for the observed reduction of the magnetic moments from CeCu to $CeNi_{0.4}Cu_{0.6}$ important modifications of the CEF level scheme must be considered. However, this circumstance is, in fact, quite unusual considering the small

Table 2. Summary of the magnetic structure data for the $CeNi_{1-x}Cu_x$ series: T indicates the temperature at which the experiment was performed, $\mathbf{q}$ is the propagation vector, structure type indicates the magnetic character and the magnetic moment orientation, μ is the magnetic moment modulus and ϕ_i represents the angles of the magnetic moments with the **a**-axis for the four 4*c* equivalent positions of the Ce^{3+} ions in the FeB type structure.

x	T(K)	$\mathbf{q}$	structure type	$\mu(\mu_B)$	ϕ_i(degrees)	R_{Bragg}(%)
0.6	0.1	0	Fy	0.6	-	14
0.8	0.1	0, $\|\mathbf{q}_2\|$=0.3 Å^{-1}	Conical	-	-	-
0.9	0.1	(1/2,0,0)	AFM(**xz**)	1.0	314, 12, 8, 100	26
0.9	0.1	(0,1/2,0)	AFM(**xy**)	1.0	144, 91, 324, 72	29
1	2	(1/2,0,0)	AFM(**xz**)	1.45	323, 16, 351, 120	12

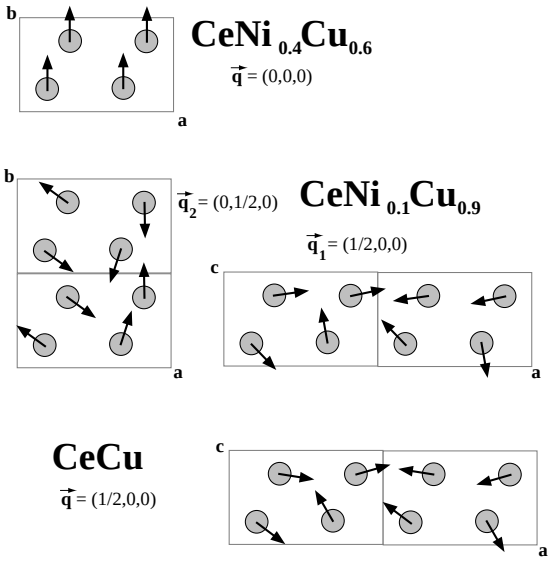

Fig. 3. Sketch of the evolution of the magnetic moment arrangement in $CeNi_{1-x}Cu_x$ within the ordered state (x = 0.6, 0.9 and 1.0) as determined by neutron diffraction. Ni/Cu ions are omitted for clarity.

changes on the cell volume and so this possibility must be discarded.

On the other hand, the reduction of the magnetic moments due to the Kondo interaction is correlated to the ratio between the Kondo temperature and the exchange energy (*e.g.*, for $CeCu_5$ [25], with T_K = 2.2 K and T_N = 3.9 K, the estimated reduction due to Kondo effect is about 15%). In our case, T_K = 2 K (see Sect. 4) and T_c = 1.1 K for x = 0.6; then, a larger reduction is expected. From these results we can ascertain that the reduction of the magnetic moments when increasing the Ni content is mainly due to the progressive Kondo screening. However, the obtained magnetic moment for x = 0.6 is 1/3 of the value found in the CeCu compound where hybridisation effects were not detected and the existence of a small spin glass component below T_c, as was suggested in [23], should not be discarded. Recent neutron experiments on a bulk sample [26] indicate that the spin glass phase could coexist below T_c with a long-range magnetic order. In order to verify this idea further experiments are needed.

We shall now comment the evolution of the magnetic structures displayed in Figure 3. The extreme studied compositions, x = 0.6 and x = 1, present simple FM and AFM structures with a single propagation vector. It seems clear that for the Ni rich ferromagnetic compounds, the easy magnetisation direction is the **b**-axis, as was also observed in the pseudobinary isomorphous compound $GdNi_{0.7}Cu_{0.3}$ [27], while for the AFM CeCu the moments lie in the **ac** plane. The intermediate compositions reflect the evolution from one situation to another. In fact, for x = 0.8 the magnetic structure keeps a FM component, but an AFM one develops associated with an incommensurate propagation vector $|\mathbf{q}_2|$ = 0.30 Å^{-1}. For x = 0.9, one of the propagation vectors appearing in the magnetic diffraction pattern, $\mathbf{q}_1$=(1/2,0,0), corresponds to that associated with the magnetic structure of CeCu (see Fig. 3 and Tab. 2), while the other arrangement described with $\mathbf{q}_2$=(0,1/2,0) still keeps a component of the magnetic moment in the **b**-direction, probably indicating a reminiscent evolution from the ferromagnetic situation. Bearing this evolution in mind we can correlate the magnetic phase associated with a propagation vector (0,1/2,0), found in x = 0.9, with the incommensurate magnetic structure of x = 0.8. In this way, we can suggest for this latter compound, a propagation vector $\mathbf{q}_2$= (0,0.2,0) (in reciprocal lattice units), leading to $|\mathbf{q}_2|$ = 0.30 Å^{-1} with a magnetic moment component along the **b**-direction. This means that the antiferromagnetism appears through an incommensurate phase which tends to take the magnetic moments out of the **b**-direction favouring the **ac** plane as the easy magnetisation one for CeCu. The complex magnetic structures of the intermediate compounds reflect the strong competition of positive and negative interactions and the changes in the anisotropy, induced by the Ni substitutions through the modification of the conduction band.

4 Quasielastic neutron scattering (QENS)

4.1 Experimental results

The differential cross-section for magnetic neutron scattering can be written as

$$\frac{\mathrm{d}^2\sigma}{\mathrm{d}\Omega \mathrm{d}(\hbar\omega)} \propto \frac{k_1}{k_0} S(Q,\omega,T), \qquad (1)$$

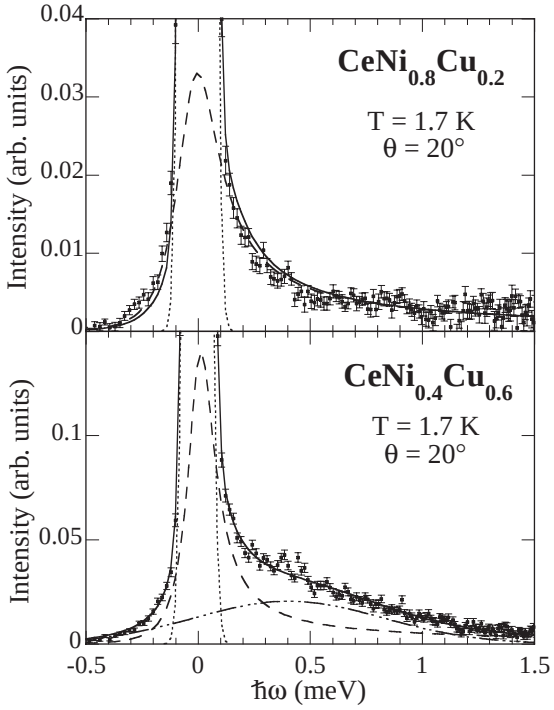

Fig. 4. Inelastic neutron scattering spectra measured at 1.7 K and $\theta = 20°$ for $CeNi_{0.8}Cu_{0.2}$ and $CeNi_{0.4}Cu_{0.6}$ compounds. Full line represents a fit to the three contributions: Elastic Gaussian (dotted line), Quasielastic Lorentzian (dashed line) and Inelastic Gaussian (dashed and dotted line).

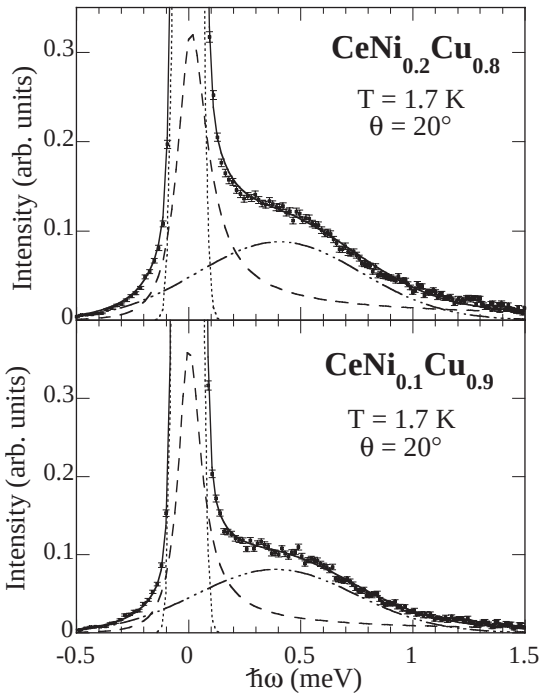

Fig. 5. Inelastic neutron scattering spectra measured at 1.7 K and $\theta = 20°$ for the $CeNi_{0.2}Cu_{0.8}$ and $CeNi_{0.1}Cu_{0.9}$ compounds. Symbols have the same meaning as in Figure 4.

where $\mathbf{k}_0$ and $\mathbf{k}_1$ are the incident and final neutron wave vectors, and $\hbar\mathbf{Q}=\hbar(\mathbf{k}_0-\mathbf{k}_1)$ and $\hbar\omega$ are the momentum and energy transfer, respectively. The magnetic scattering function $S(Q,\omega,T)$ for the quasielastic contribution can be written assuming that the excitation spectrum is approximated to a simple relaxation process with a relaxation rate $\Gamma/2$, corresponding to the halfwidth at half maximum of the Lorentzian observed spectra [28].

$$S(Q,\omega,T) \propto \frac{\omega}{1-\mathrm{e}^{-\frac{\hbar\omega}{k_\mathrm{B}T}}} F^2(Q) \frac{\Gamma/2}{(\Gamma/2)^2+(\hbar\omega)^2} \chi'(Q,0,T) \tag{2}$$

with $F(Q)$ the magnetic form factor and $\chi'(Q,0,T)$ the real part of the static susceptibility. Only in the absence of spatial correlations between the magnetic moments, when $\mathbf{Q}\to 0$, should the local static susceptibility $\chi'(Q,0,T)$ be similar to the static bulk susceptibility $\chi'(0,0,T)$ as measured in a magnetometer.

In Figures 4 and 5 we present the neutron spectra measured at 1.7 K and a scattering angle $\theta = 20°$ for the studied compositions. Considering the dependence with the scattering angle, no phonon contribution is detected in the range 0–2 meV. Furthermore, the isomorphous non-magnetic YNi compound does not show any trace of phonon contributions in this energy range [24]. In addition, no CEF excitations are detected in this energy range, according to the analysis of the specific heat measurements [23]. From these results it was deduced that the first CEF level should appear at much higher energies in this series of compounds.

For all the samples, the neutron scattering response can be fitted considering an Elastic Gaussian-shape nuclear contribution (EG) and a Quasielastic Lorentzian-shape term (QL) modified by the detailed balance factor as in formula (2). Additionally, for compositions with $x \geq 6$, in order to account for the experimental spectra, an extra Inelastic Gaussian-shape contribution (IG), centred on 0.5 meV, is needed. In the analysed range ($20° < \theta < 60°$) this contribution is almost independent for a fixed temperature. When increasing the temperature, this IG excitation shifts to lower energies, broadening and decreasing in intensity. Finally, it disappears for $T > 10$ K, well above the ordering temperature. The origin of this contribution will be discussed later.

Using $\Gamma/2$ and the amplitudes of EG and QL (and IG) as adjustable parameters we obtain a reasonably good fit for all the $CeNi_{1-x}Cu_x$ spectra as shown by the solid line in Figures 4 and 5. The $\Gamma/2$ of the quasielastic contribution increases with increasing temperature. This temperature dependence of $\Gamma/2$ is shown in Figure 6. For $CeNi_{0.1}Cu_{0.9}$ and $CeNi_{0.2}Cu_{0.8}$ a linear behaviour (Korringa law) is found, as usually appears for Kondo lattice compounds with long-range magnetic order [1,2]. For the composition with $x = 0.6$, it is very difficult to establish a clearly linear or $T^{1/2}$ dependence. From the linear fits, a Kondo temperature is estimated as $\lim_{T\to 0} \frac{\Gamma/2}{k_\mathrm{B}}$.

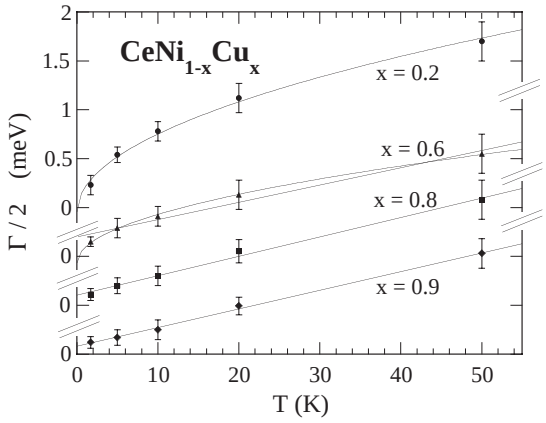

Fig. 6. Temperature variation of $\Gamma/2$ for the $CeNi_{1-x}Cu_x$ series. Lines are fits to linear or $T^{1/2}$ dependences (see text). The vertical scale has been shifted for the sake of clarity.

The obtained values are 2 K, 1 K and 0.7 K for $x = 0.6$, 0.8 and 0.9, respectively.

The $CeNi_{0.8}Cu_{0.2}$ compound presents larger $\Gamma/2$ values and a clear $T^{1/2}$ dependence, as usually observed in heavy fermion compounds [1,2]. The evolution of the $\Gamma/2$ values through the series and their thermal variation reflect the increasing hybridisation effects when the Cu concentration decreases. For the $CeNi_{0.8}Cu_{0.2}$ compound, in order to estimate T_K from the deviation from the $T^{1/2}$ dependence, more low temperature data are needed, as it has been done in $CeAl_2$ [29] or $CeCu_6$ [30,31].

4.2 Discussion on QENS

Although several reviews have been devoted to the inelastic neutron scattering in heavy fermions and related compounds [1,2], the large phenomenology and the description of many particular cases make it very difficult to generalise in a simple way the contrast between theory and experiment. However, the existence of a quasielastic excitation is a common signature of the $4f$-conduction band hybridisation (Kondo effect), and some general trends about its intensity, temperature and Q dependence are related to the nature of the ground state level of the mentioned compounds. In this way, many efforts have been made to account for those dependences and, in particular the neutron scattering spectrum considering an effective resonant-scattering Hamiltonian including both Kondo and CEF effects has been calculated by Lopes and Coqblin [11] and Fulde and Loewenhaupt [12]; both authors found a linear Korringa law for the temperature variation of $\Gamma/2$ such as $\Gamma/2 \propto |n(E_F)\Im|^2 T$ where $n(E_F)$ and $\Im$ are the density of states of the conduction band at the Fermi level and the exchange integral, respectively. The application of these calculations implies the existence of a net magnetic moment as well as Kondo interactions and non-negligible CEF. In this situation are included the Kondo lattice compounds, with competing long-range magnetic order and $4f$-conduction band hybridisation. This linear variation of $\Gamma/2$ has been found in $CeMg_3$ [9] ($T_N = 3.4$ K), $CeCu_2$ [32] ($T_N = 3.5$ K) and $CeNi_{1-x}Pt_x$ [10] ($T_c < 8$ K), among others.

In the case of dominating Kondo interactions, the compounds do not usually present long-range magnetic order and the theoretical approaches are developed in the framework of spin fluctuations [33,34]. These models predict a $\Gamma/2$ finite value at 0 K proportional to the spin fluctuation temperature T_{SF}, following a $T^{1/2}$ law at higher temperatures. Bickers *et al.* found the same $T^{1/2}$ dependence for $T > T_K$ considering the single impurity Anderson model in the non-crossing terms approximation [13]. Several heavy fermion compounds such as $CeCu_2Si_2$ [7], $CeCu_6$ [30,31] and $CeAl_2$ [29] present this $T^{1/2}$ variation. In all these systems the QE lines are wider than those of the compounds following the Korringa law.

Our experimental results show a clear increase in the $\Gamma/2$ value with the increasing Ni concentration, indicating the enhancement of the Kondo interactions. A linear $\Gamma/2$ *vs.* T behaviour is found for the $x = 0.9$ ($T_N = 2.5$ K) and 0.8 ($T_c = 1.2$ K) compounds. For these compounds the magnetic RKKY interactions are preponderant with respect to the Kondo effect and the QE data can be understood considering the effective resonant scattering Hamiltonian. In contrast, for $CeNi_{0.8}Cu_{0.2}$, where no long-range magnetic order has been found down to 1 K, a $T^{1/2}$ law was obtained according to the most important role of Kondo interactions. The $CeNi_{0.4}Cu_{0.6}$ compound shows a very interesting behaviour: in fact, this compound has been characterised as a ferromagnet with $T_c = 1.1$ K, but with a strong influence of the hybridisation (very reduced magnetic moments, as commented in Sect. 3). For this composition, the unclear $\Gamma/2$ behaviour (as commented in Sect. 4.1), reflects the evolution from a magnetic ground state to a non-magnetic one. A similar feature was also detected in $CeRu_2Si_2$ [35], which is a compound on the border between heavy fermion and intermediate valence behaviour. In this case, the almost linear variation of $\Gamma/2$ is related to some surviving ferromagnetic correlations. In our case, for $CeNi_{0.4}Cu_{0.6}$, the incipient curvature in the $\Gamma/2$ thermal variation is a signature of the increasing importance of the Kondo effect.

In order to account for the experimental spectra of the magnetically ordered $CeNi_{1-x}Cu_x$ compounds ($x \geq 0.6$), an additional IG term has to be considered. This supplementary excitation centred around 0.5 meV persists up to 10 K and its intensity increases when the exchange interaction becomes more important (increasing Cu percentage). The main characteristics of this inelastic excitation (full width at half maximum, Σ, and energy position, ϵ) are gathered in Table 3. The Σ value increases slightly and ϵ shifts to lower energies on increasing the temperature. This behaviour cannot be attributed to phonon or CEF excitations, but it is probably due to spin-spin correlations between Ce ions, which remain well above the ordering temperature. This situation is reminiscent of the case of $CeCu_2$ in which a similar excitation was observed up to 50 K, while the ordering temperature was only 3.5 K [32].

Table 3. Full width at half maximum (Σ) and energy position (ϵ) of the inelastic (Gaussian) contribution to the neutron spectra at different temperatures in the $CeNi_{1-x}Cu_x$ series.

	$x = 0.6$		$x = 0.8$		$x = 0.9$	
T(K)	Σ(meV)	ϵ(meV)	Σ(meV)	ϵ(meV)	Σ(meV)	ϵ(meV)
1.7	1.00(4)	0.40(1)	0.82(2)	0.36(1)	0.84(2)	0.39(1)
5	1.04(6)	0.24(3)	0.92(2)	0.20(1)	0.82(2)	0.140(5)
10	1.16(4)	0.12(2)	1.00(2)	0.096(7)	0.86(2)	0.072(3)

In contrast, similar experiments performed on the ferromagnetic $CeNi_{1-x}Pt_x$ system [10] show a magnon-like excitation below the ordering temperature but no other supplementary inelastic peak was found above T_c. Then, the actual IG contribution is interpreted as a sign of the competing positive and negative magnetic interactions which tends to keep a short-range magnetic order above T_c.

5 General discussion and conclusions

The pseudobinary compounds $CeNi_{1-x}Cu_x$ present a complex situation from the point of view of the modification of both the RKKY interaction (changes from FM to AFM behaviour) and the Kondo effect (crossover from long-range magnetic order to non-magnetic behaviour). These evolutions, previously characterised by macroscopic measurements [15,16,21], are now studied by neutron scattering techniques, giving a better insight into the microscopic mechanisms which are at the origin of the complex macroscopic magnetic behaviour.

From the analysis of the magnetic structures we can conclude that, while CeCu is AFM with the magnetic moments in the **ac** plane, the introduction of Ni favours the FM interactions and leads the easy magnetisation axis in the **b**-direction (notice the $CeNi_{0.4}Cu_{0.6}$ magnetic structure). The intermediate structures are understood as the result of the progressive evolution between these two simple structures. In this way, although the negative interactions are not dominant for the FM compounds, they are still present. Then, the spin glass like state appearing in these compounds [21] could be a memory of the antiferromagnetic ordering, probably coexisting with the ferromagnetic component along the **b**-direction. This possibility is supported by the very small value of the Ce^{3+} magnetic moment (μ_{Ce}=0.6 μ_B) found in $CeNi_{0.4}Cu_{0.6}$ and the existence of spin-spin correlations evidenced from the IG excitation in the QENS spectra.

In addition, the evolution of the Kondo temperature obtained from QENS indicates that the $4f$-conduction band hybridisation increases with the Ni content, in agreement with previous macroscopic estimates [15,16]. These effects are mainly driven by the evolution of interatomic distances, as was also observed in $CeNi_{1-x}Pt_x$ [20]. As usually occurs, the T_K values estimated from QENS are smaller than those obtained from macroscopic measurements [15,16] due to the different time scales of each experimental technique.

One of the features making this system especially relevant is that the Kondo and the ordering temperatures are quite similar in magnitude. This fact allows us to follow the change of regime in the temperature dependence of $\Gamma/2$. The evolution from a linear Korringa law to a $T^{1/2}$ variation indicates the continuous increase of the hybridisation effects and the progressive reduction of the RKKY type exchange interactions. In this way, our series provides a model system where neutron scattering data show this continuous evolution driven by chemical substitutions. Although these results are compared with different theoretical models [11–13,33,34], we must keep in mind that they use different approaches. Then, a global understanding of the experimental results would require a unified model where RKKY, CEF and Kondo interactions were considered at the same level and could be tuned depending on their relative importance.

In conclusion, this system shows a variety of magnetic structures such as ferromagnetic, conical and antiferromagnetic which are consequence of the competing exchange interactions (positive and negative) combined with the Kondo screening. Moreover, the insight of the QENS results on the Kondo characteristic of this series provides direct evidence of the continuous evolution of the $4f$-conduction band hybridisation strength and the existence of spin-spin correlations above the magnetic ordering temperature.

We are indebted to L. Echeandia, S. Pujol and H. Buttner for their help during the experiments. This work was partially supported by the CICYT, project MAT99-0667 and the ESF, program FERLIN.

References

1. M. Loewenhaupt, K.H. Fischer, in *Handbook of Magnetic Materials*, edited by K.H.J. Buschow (North Holland, Amsterdam, 1993), Vol. 7, p. 503.
2. E. Holland-Moritz, G.H. Lander, in *Handbook on the Physics and Chemistry of Rare Earths*, edited by K.A. Gschneidner Jr, L. Eyring, G.H. Lander, G.R. Choppin (North Holland, Amsterdam, 1995), Vol. 19, p. 1.
3. J.C. Gómez Sal, J.A. Blanco, J.I. Espeso, J. Rodríguez Fernández, J. Rodríguez Carvajal, Solid State Commun. **87**, 863 (1993).
4. E. Holland-Moritz, M. Loewenhaupt, W. Schmatz, D.K. Wohlleben, Phys. Rev. Lett. **38**, 983 (1977).

5. E. Holland-Moritz, D. Wohlleben, M. Loewenhaupt, Phys. Rev. B **25**, 7482 (1982).
6. A.P. Murani, K. Knorr, K.H.J. Buschow, A. Benoit, J. Flouquet, Solid State Commun. **36**, 523 (1980).
7. S. Horn, E. Holland-Moritz, M. Loewenhaupt, F. Steglich, H. Scheuer, A. Benoit, J. Flouquet, Phys. Rev. B **23**, 3171 (1981).
8. S. Horn, F. Steglich, M. Loewenhaupt , H. Scheuer, W. Felsch, K. Winzer, Z. Phys. B **42**, 125 (1981).
9. J. Pierre, A.P. Murani, R.M. Galera, J. Phys. F **11**, 679 (1981).
10. J.A. Blanco, J. Sandonís, J. Rodríguez-Fernández, J.C. Gómez Sal, F. Plazaola, J.M. Barandiarán, in *Quasielastic Neutron Scattering*, edited by J. Colmenero, A. Alegría, F.J. Bermejo (World Scientific, Singapore, 1994), p. 211; J.A. Blanco, J.C. Gómez Sal, J. Rodríguez-Fernández, J. Sandonís, J.M. Barandiarán, Physica B **100-101**, 217 (1992).
11. L.C. Lopes, B. Coqblin, Phys. Rev. B **38**, 6807 (1988).
12. P. Fulde, M. Loewenhaupt, Adv. Phys. **34**, 589 (1986).
13. N.E. Bickers, D.L. Cox, J.W. Wilkins, Phys. Rev. B **36**, 2036 (1987).
14. D. Gignoux, D. Givord, R. Lemaire, F. Tasset, J. Less-Common Met. **94**, 165 (1983).
15. J. García Soldevilla, J.C. Gómez Sal, J. Rodríguez Fernández, J.I. Espeso, L. Monconduit, J. Allemand, D. Paccard, Physica B **230-232**, 117 (1997).
16. J. García Soldevilla, J.C. Gómez Sal, J.I. Espeso, J. Rodríguez Fernández, J.A. Blanco, M.T. Fernández Díaz, H. Buttner, J. Magn. Magn. Mater. **177**, 300 (1998).
17. D. Gignoux, J.C. Gómez Sal, J. Magn. Magn. Mater. **1**, 203 (1976).
18. J. García Soldevilla, J.C. Gómez Sal, J. Rodríguez Fernández, J.I. Espeso, M.A. Argüelles, J. Magn. Magn. Mater. **186**, 49 (1998).
19. J. García Soldevilla, J.I. Espeso, J. Rodríguez Fernández, J.C. Gómez Sal, J.A. Blanco, P. Galez, D. Paccard, J. Magn. Magn. Mater. **157-158**, 624 (1996).
20. D. Gignoux, J.C. Gómez Sal, Phys. Rev. B **30**, 3967 (1984).
21. J. García Soldevilla, J.C. Gómez Sal, J.A. Blanco, J.I. Espeso, J. Rodríguez Fernández, Phys. Rev. B **61**, (2000) 6821.
22. J. Rodríguez Carvajal, Physica B **192**, (1993) 55.
23. J.C. Gómez Sal, J. García Soldevilla, J.A. Blanco, J.I. Espeso, J. Rodríguez Fernández, F. Luis, F. Bartolomé, J. Bartolomé, Phys. Rev. B **56**, 11741 (1997).
24. J. García Soldevilla, J.I. Espeso, J.A. Blanco, J.C. Gómez Sal, P. Galez, D. Paccard, J. Rodríguez-Carvajal, B. Ouladdiaf, Physica B **234-236**, 758 (1997).
25. E. Bauer, M. Rotter, L. Keller, P. Fischer, M. Ellerby, K.A. McEwen, J. Phys. Cond. Matt. **6**, 5533 (1994).
26. J.C. Gómez Sal, J. Rodríguez Fernández, J.I. Espeso, N. Marcano, J.A. Blanco, presented to ICM'2000 (to be published in J. Magn. Magn. Mater.).
27. J.A. Blanco, J.C. Gómez Sal, J. Rodríguez-Fernández, D. Gignoux, D. Schmitt, Rodríguez-Carvajal, J. Phys. Cond. Matt. **4**, 8233 (1992).
28. E. Holland-Moritz, M. Loewenhaupt, W. Schmatz, D.K. Wohlleben, Phys. Rev. Lett. **38**, 983 (1977).
29. S. Horn, F. Steglich, M. Loewenhaupt, E. Holland-Moritz, Physica B **107**, 103 (1981).
30. U. Walter, D. Wohlleben, Z. Fisk, Z. Phys. B **62**, 325 (1986).
31. J. Rossat-Mignod, L.P. Regnault, J.L. Jacoud, C. Vettier, P. Lejay, J. Flouquet, E. Walker, D. Jaccard, A. Amato, J. Magn. Magn. Mater. **76-77**, 376 (1988).
32. M. Loewenhaupt, E. Gratz, N. Pillmayr, H. Mller, Physica B **163**, 427 (1990).
33. C.M. Varma, *U.S.-Japan Seminar on: Physical Properties of Rare-Earth Magnetic Semiconductors* (Sendai, October 1997) p. 56.
34. L.C. Lopes, Y. Lassailly, R. Julien, B. Coqblin, J. Magn. Magn. Mater. **31-34**, 251 (1983).
35. A. Severing, E. Holland-Moritz, B. Frick, Phys. Rev. B **39**, 41 (1989).